



Original article

Glucal-conjugated sterols as novel vascular leakage blocker: Structure–activity relationship focusing on the C₁₇-side chain



Kyeojin Kim^{a,1}, Sony Maharjan^{b,1}, Changjin Lim^a, Nam-Jung Kim^c, Vijayendra Agrawal^b, Young Taek Han^d, Sujin Lee^a, Hongchan An^a, Hwayoung Yun^a, Hyun-Jung Choi^b, Young-Guen Kwon^{b,**}, Young-Ger Suh^{a,*}

^a College of Pharmacy, Seoul National University, 1 Gwanak-ro, Gwanak-gu, Seoul 151-742, Republic of Korea

^b Department of Biochemistry, College of Life Science and Biotechnology, Yonsei University, Seoul 120-749, Republic of Korea

^c Department of Pharmacy, College of Pharmacy, Kyung Hee University, Seoul 130-701, Republic of Korea

^d College of Pharmacy, Woosuk University, Wanju 565-701, Republic of Korea

ARTICLE INFO

Article history:

Received 27 August 2013

Received in revised form

8 January 2014

Accepted 14 January 2014

Available online 25 January 2014

Keywords:

Anti-apoptotic agents

Tight junction

Pregnenolone

Oxime

Ginsenoside Rk1

Diabetic retinopathy

ABSTRACT

A series of glucal-conjugated sterols as novel vascular leakage blocker were identified through design, synthesis and biologically evaluation. In addition, the structure-activity relationship (SAR) of the glucal-conjugated sterols focusing on the C₁₇-side chain was also established. The sterol analogs linked with the rigid C₁₇-side chain side chains exhibited potent cell survival activities. In particular, analog **211**, which possesses a cyclopentyl oxime moiety, was shown to have excellent pharmacological effects on retinal vascular leakage in a diabetic mouse model.

© 2014 Elsevier Masson SAS. All rights reserved.

1. Introduction

The endothelium is a thin layer of endothelial cells, which constitute the inner lining of blood vessels and form an interface between circulating blood in the lumen and rest of the vessel wall. The disintegration of the endothelium causes pathological symptoms such as diabetic retinopathy, which is a complication that occurs primarily in patients with diabetes mellitus [1]. Vascular leakage can be caused by the disruption of tight junctions between

endothelial cells and the collapse of endothelial cell homeostasis [1–4]. Homeostasis at the vascular cell level is maintained by an appropriate balance between cell proliferation and apoptosis [5,6]. In particular, the excessive apoptosis of vascular endothelial cells (VECs) can disrupt the integrity of vessels and the normal function of the endothelium [7,8]. The loss of integrity and vascular permeability lead to a macular edema, which is normally accompanied by diabetic retinopathy [9,10]. Nevertheless, there has been little progress in the treatment of vascular leakage despite clinical trials of small molecules such as calcium dobesilate, aspirin, and antihistamines [1]. Laser surgery still remains the primary treatment for vascular leakage [11]. Consequently, medications for the treatment of retinal vascular leakage are still urgently needed.

We reported the potent anti-apoptotic activities of ginsenosides Rg3 (**1**) and Rk1 (**2**), which were isolated from the root of ginseng, in human umbilical vein endothelial cell (HUVEC) lines [12]. We also reported the identification of novel anti-apoptotic agents, including SAC-0504 (**3**) and SAC-0601 (**4**), that consist of a cholesterol scaffold and a carbohydrate equivalent, in place of the protopanaxadiol backbone and the carbohydrate, respectively, of Rk1 [13] (Fig. 1).

Abbreviations: HUVEC, human umbilical vein endothelial cell; TJs, tight junction; PTSA, *para*-toluenesulfonic acid; DHP, 3,4-dihydro-2H-pyran; DBU, 1,8-Diazabicyclo[5.4.0]undec-7-ene; HREC, human retina endothelial cell; MTT, (3-(4,5-dimethylthiazol-2-yl)-2,5-diphenyltetrazolium bromide; VEGF, vascular endothelial growth factor; BRB, blood-retinal barrier.

* Corresponding author. Tel.: +82 2 880 7875; fax: +82 2 888 9122.

** Corresponding author. Tel.: +82 2 2123 5697; fax: +82 2 362 9897.

E-mail addresses: ygkwon@yonsei.ac.kr (Y.-G. Kwon), ygsuh@snu.ac.kr (Y.-G. Suh).

¹ These authors contributed equally to this work.

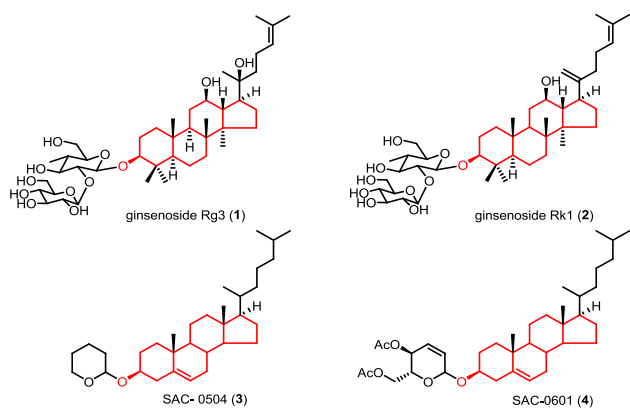


Fig. 1. Natural and synthetic sterol analogs.

SAC-0601 exhibited not only potent anti-apoptotic activity but also a protective effect against the disruption of tight junctions (TJs) which leads to retinal vascular leakage [13,14]. Therefore, the further development of chemotherapeutically useful sterol analogs for the treatment of diabetic retinopathy was quite attractive to us because of the high demand for drugs that maintain endothelial integrity and because of the excellent protective effects of these sterol analogs, which were previously identified by us, for the endothelial system [13–15].

Furthermore, we reported the anti-apoptotic activities of the carbohydrate equivalent-linked analogs of phytosterols including sitosterol, sitostanol and stigmasterol [16]. Interestingly, the activities of these compounds depended on the C₁₇-side chain attached to the D-ring of the phytosterols. These results also revealed that the branched alkyl chain of the phytosterol plays an important role in determining the biological activities. Thus, we designed second-generation sterol analogs linked to carbohydrate equivalent, 4,6-di-O-acetyl-2,3-dideoxyhex-2-enopyran. Our strategy focused on the C₁₇-side chain modification of SAC-0504 (3) and SAC-0601 (4) based on the structures of ginsenosides Rg3 (1) and Rk1 (2), which have *tert*-alcohol and *exo*-olefin in the C₁₇-side chain, respectively. We initially investigated the effect of *tert*-alcohol on the assumption that *tert*-alcohol can be transformed to the *endo/exo*-olefin via dehydration. In addition, we further modified the C₁₇-side chain by incorporating oxime ether because we anticipated that the constrained conformation would provide improved binding affinity to the target protein [17–19]. Insertion of heteroatom was also anticipated to reduce the high lipophilic character of the analogs. Thus, commercially available pregnenolone (9) was selected as an appropriate substrate for synthesis of the newly designed analogs in terms of accessibility and synthetic efficiency (Fig. 2).

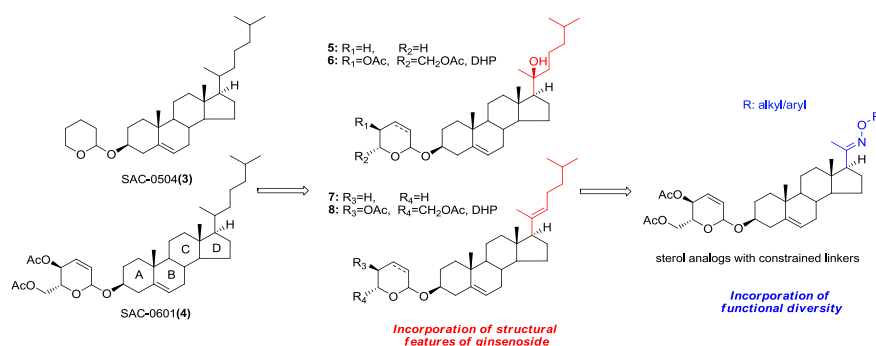


Fig. 2. Strategy for the development of novel sterol analogs based on SAC-0601.

2. Results and discussion

2.1. Chemistry

2.1.1. Synthesis of the glucal conjugated sterols with modified C₁₇-side chain based on the structures of ginsenosides Rg3 (1) and Rk1 (2)

The analogs of 3 and 4 with the modified C₁₇-side chains were synthesized from 9 as outlined in Scheme 1. The tetrahydropyran analog 5, which possesses a *tert*-alcohol in the side chain, was prepared by the reaction of 9 with dihydropyran in the presence of PTSA, followed by a diastereoselective Grignard reaction [20]. The dihydropyran analog 6 was synthesized via Grignard reaction and subsequent glycosidation with *tri*-O-acetyl-D-glucal [13,21]. We also synthesized pyran-linked analogs with side chains that are structurally similar to that of ginsenoside Rk1 (2). The elimination of the *tert*-alcohol of analog 5 using Et₃N and MsCl produced *regio*/stereoisomers of 12, 14 which could not be separated by column chromatography. Other analogs with side chains possessing double bonds were conveniently prepared from the common intermediate 15, which was prepared by the Wittig olefination [22] of 9. Analog 7 was synthesized by the reaction of 15 with DHP in the presence of PTSA. The reaction of *tri*-O-acetyl-D-glucal with intermediate 15 in the presence of BF₃·OEt₂ in THF provided analog 8.

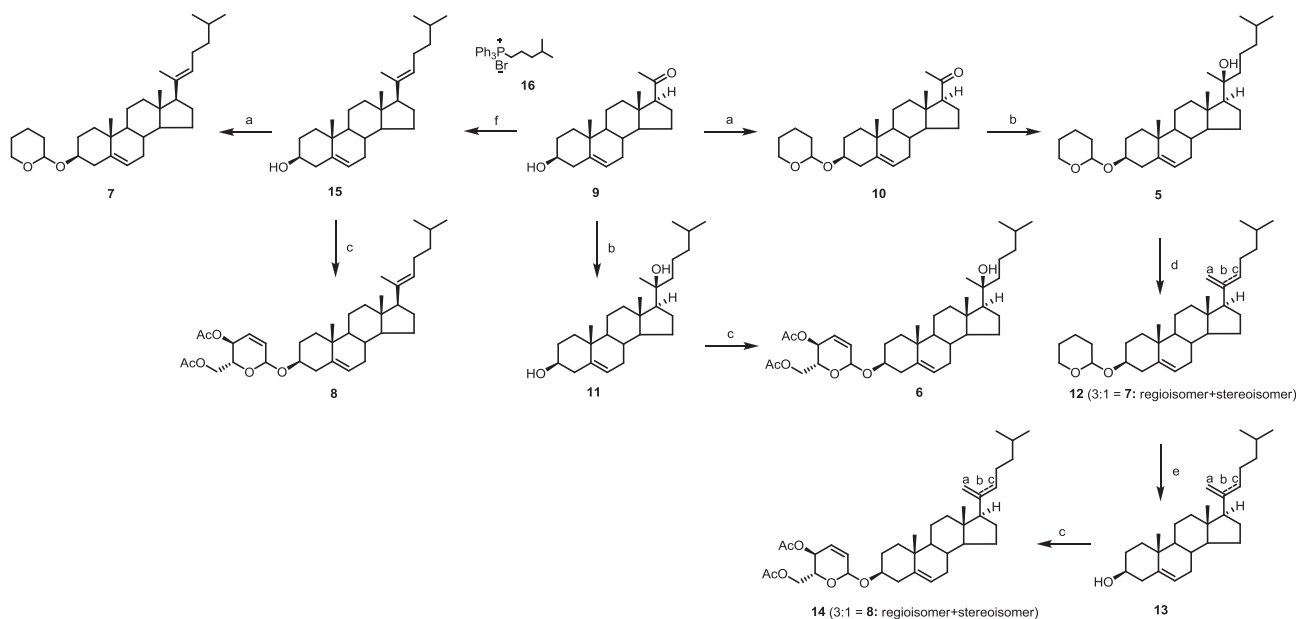
2.1.2. Synthesis of the glucal-conjugated oxime analogs

Next, we prepared a variety of oxime ether analogs as variants of the olefin-possessing analog 8. Initially, various hydroxyl amines were prepared as described in Scheme 2. Most hydroxylamine·HCl salts could be prepared from commercially available *N*-hydroxyphthalimide (17), which was transformed into alkoxypthalimides 18a–p using DBU and the corresponding alkyl halide [23] or by the Mitsunobu reaction [24] in the presence of the corresponding alkyl alcohols. Sequential imide cleavage of the resulting imides using methyl hydrazine followed by hydrochloride salt formation afforded 19a–p [18,23,24]. With the requisite alkyloxyamine salts and the commercially available hydroxylamine·HCl and benzylhydroxylamine·HCl salts in hand, we were able to synthesize oxime analogs via a unified synthetic strategy [17–24]. The reaction of *tri*-O-acetyl-D-glucal with 9 provided the key intermediate 20, which was transformed into a variety of glucal-conjugated oxime analogs (21a–r) by condensation with the corresponding hydroxylamine·HCl salts in refluxing pyridine.

2.2. Biology

2.2.1. In vitro assay

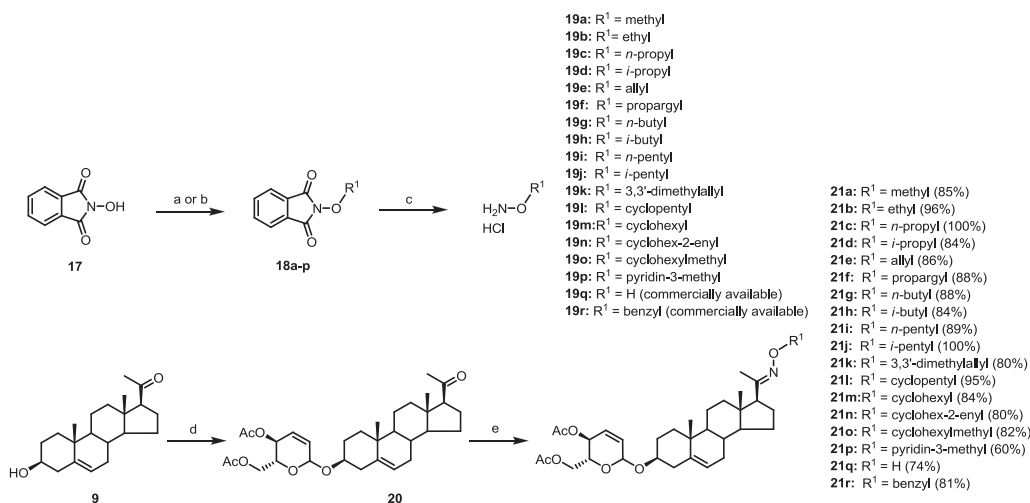
Given that apoptosis is generally associated with the onset of diabetic retinopathy [25,26], we investigated the anti-apoptotic



Scheme 1. Synthesis of the glucal conjugated sterols with modified C₁₇-side chain based on the structures of ginsenosides Rg3 (**1**) and Rk1 (**2**). Reagents and conditions: (a) PTSA, DHP, CH₂Cl₂, 57%; (b) Mg turning, 1-bromo-4-methyl pentane, Et₂O, 15–18%; (c) *tri*-*O*-acetyl-*D*-glucal, BF₃·OEt₂, THF, 12–23%; (d) Et₃N, MsCl, CH₂Cl₂, 40%; (e) PTSA, MeOH, 99%; (f) *t*-BuOK, **16**, benzene, reflux, 22%.

effect of the synthesized analogs using serum-deprived human retina endothelial cells (HRECs). The anti-apoptotic activity assay was conducted using the MTT colorimetric method at 10 μg/mL for 48 h as a preliminary study [27]. Noticeably, the 10 μg/mL DMSO stock solutions of SAC-0601 (**4**) and analogs **7** and **8** were prepared as a suspension due to poor solubility whereas analogs **5**, **6** and all oxime ethers dissolved well in DMSO, which supports the increase of solubility by an incorporation of hydroxyl group or oxime ether moiety [28]. As shown in Fig. 3, some analogs with constrained side chains exhibited more potent cell survival activities than the parent analog **4**. In particular, analogs such as **7** and **8** which possess an *endo*-olefin were more potent than the analogs that possess a *tert*-alcohol or an *exo*-olefin regardless of the carbohydrate equivalent used. This result also implied that incorporation of the constrained side chain enhances the anti-apoptotic activity. Based on the results, we focused on incorporation of oxime moiety, a bioisosteric

moiety for the *endo*-olefin group, which seems to induce an appropriate conformation of the sterol analogs for higher binding affinity and induce high solubility. As predicted, the oxime analog **21h** exhibited an activity equipotent to that of the corresponding alkyl analog **8** with improved solubility. We thoroughly investigated the effects of the alkyl substituents of the oxime moiety on the biological activities of oxime ether analogs. Generally, the oxime analogs with short or medium-sized alkyl chains, such as methyl, ethyl, isopropyl, allyl and propargyl groups, exhibited slightly low anti-apoptotic activities. In contrast, the oxime ether analogs with the butyl and pentyl substituents exhibited potent activities. The analogs with branched chains (**21h** and **21j**) were more potent than the analogs with the corresponding linear chains. The non-substituted oxime (**21q**) exhibited lower activity than **4**, and the analog with the 3,3'-dimethylallyl oxime ether **21k**, exhibited a lower potency than the corresponding saturated analog



Scheme 2. Synthesis of the glucal-conjugated oxime analogs. Reaction conditions and reagents: (a) DBU, DMF, alkyl halide, 60 °C; (b) diisopropyl azodicarboxylate, pyridine-3-methanol, PPh₃, CH₂Cl₂; (c) MeNHNH₂, CH₂Cl₂; (d) BF₃·OEt₂, 3,4,6-*tri*-*O*-acetyl-*D*-glucal, CH₂Cl₂, 60%; (e) **19a–r**, pyridine, reflux.

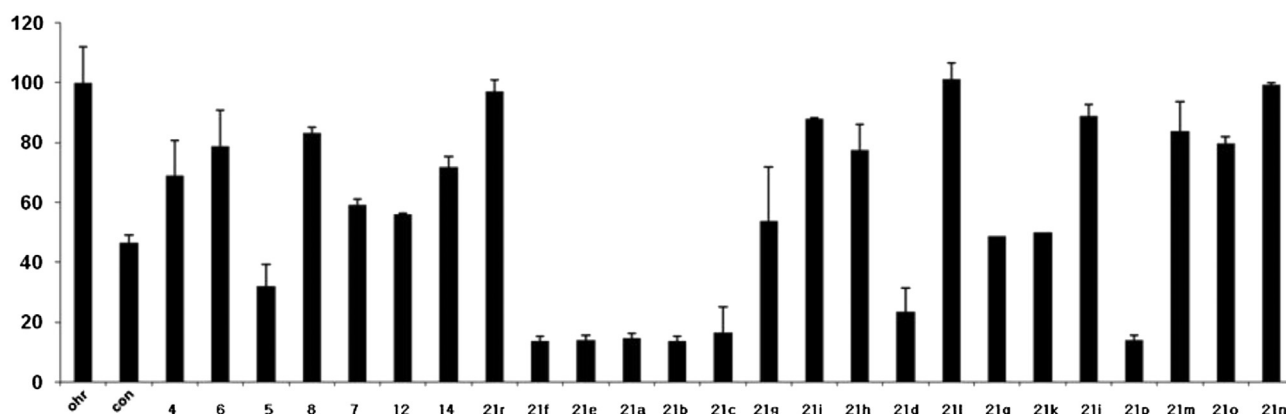
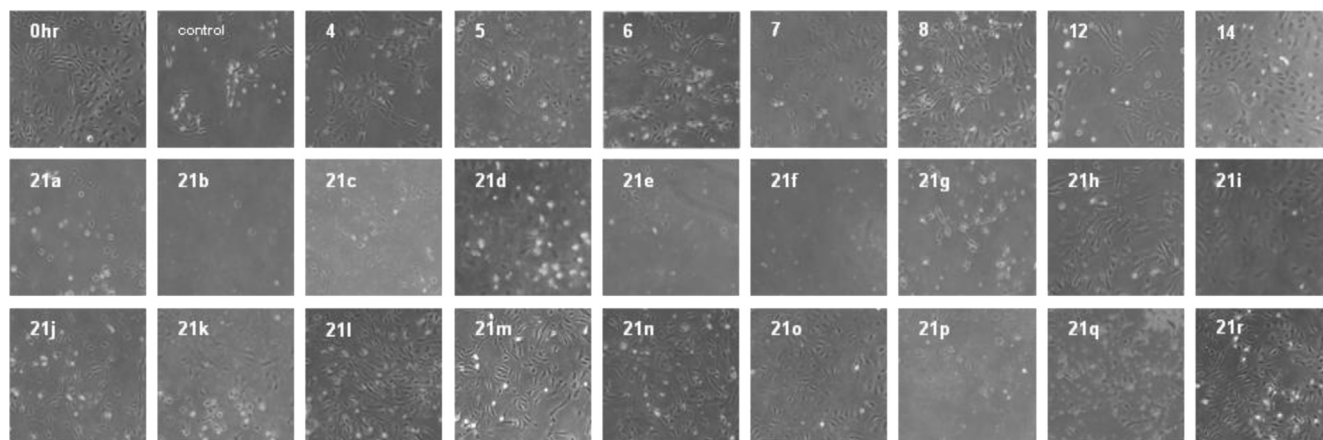


Fig. 3. Inhibitory effects of the oxime analogs on the apoptosis of HRECs. The cells were treated with 10 $\mu\text{g}/\text{mL}$ for 48 h, 0 h: the viability of the cells cultured in medium without any analog. Con: the viability of the cells cultured in medium containing DMSO used as a vehicle.

21h. Interestingly, the analogs possessing cycloalkyl oxime ethers exhibited more potent activities than oxime ether **21h** which had an acyclic alkyl substituent. The oxime ethers (**21l**, **n** and **r**) with cyclohexyl and benzyl substituents exhibited the most potent activities. However, analog **21p**, which had a heterocyclic substituent, did not have inhibitory activity [29].

Analog **21l**, **n** and **r** exhibited dose-dependent anti-apoptotic activities in the MTT assay, as shown in Fig. 4.

The oxime analogs were further tested for their protective effect against TJ disruption [14], which leads to retinal vascular leakage. These compounds were evaluated using an assay based on VEGF-induced endothelial cell permeability, which can be assessed by the formation of actin stress fibers. The blood-retinal barrier (BRB) is composed of inner (iBRB) and outer (oBRB) barriers [30]. Many clinical studies have shown that the major site that becomes permeable in diabetic retinopathy is the iBRB [14,31,32]. The iBRB is maintained by the TJs between adjacent retinal capillary

endothelial cells. These TJs are made up of many junctional proteins with intracellular partners and actin filaments, which are engaged in multiple interactions to regulate endothelial permeability [30–38]. Therefore, we used an assay that probes the actin cytoskeleton, one of the major TJ proteins in endothelial cells used to evaluate the ability of compounds to maintain the integrity of TJs [31–38]. Vascular endothelial growth factor (VEGF), which has been reported to be a key mediator of BRB collapse in diabetic retinopathy and other retinal ischemic diseases [39–42], was utilized to disrupt the stability of TJ proteins and to alter the actin filament distribution [30]. A preliminary assay using analogs **6** and **8** showed clear reductions in the formation of actin stress fibers at concentrations of 10–20 $\mu\text{g}/\text{mL}$. Accordingly, other oxime ether analogs were evaluated at a concentration of 10 $\mu\text{g}/\text{mL}$. Interestingly, analogs **21l**, **n** and **r**, which exhibited potent anti-apoptotic activities, also significantly reduced the formation of the stress fibers in HRECs, consequently leading to the stabilization of the

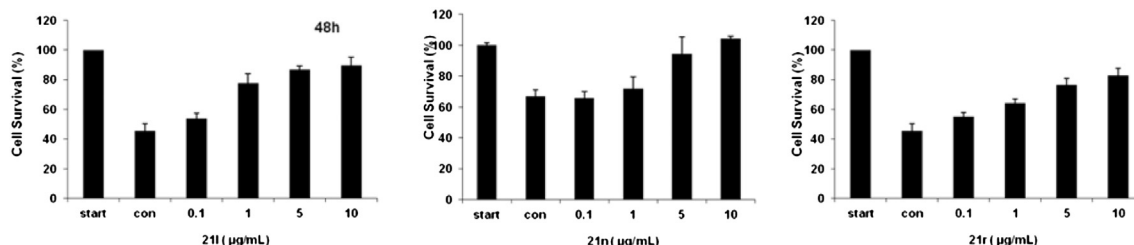


Fig. 4. Dose-dependent inhibitory effects of **21l**, **n**, and **r** on the apoptosis of HRECs. Cells were treated with concentrations from 0.1 to 10 $\mu\text{g}/\text{mL}$ for 48 h.

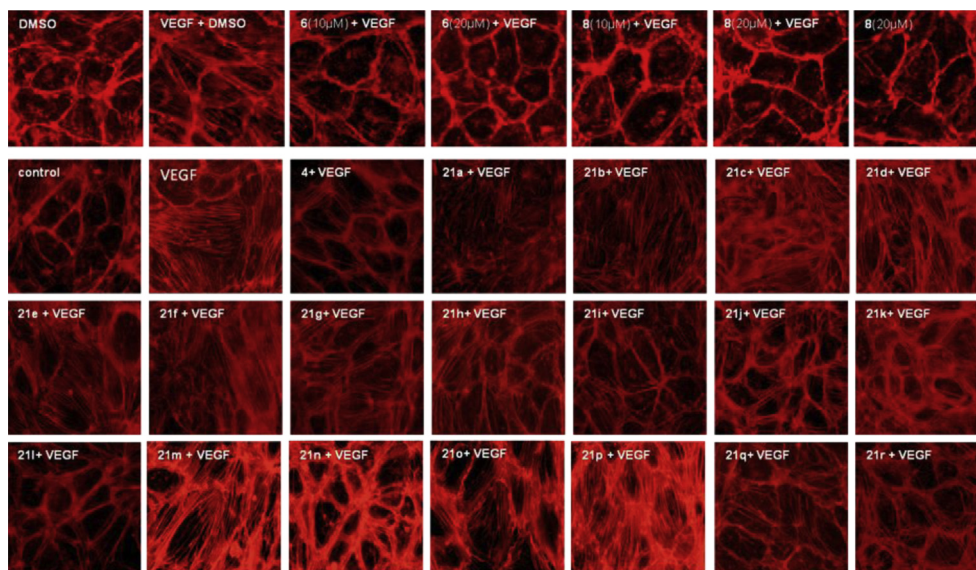


Fig. 5. Assay of oxime analogs based on the stabilization of the cortical actin ring in HRECs. HRECs were cultured on gelatin-coated dishes for 3 days. Confluent cells were serum-starved in the serum-free media for 3 h, and then pretreated with analogs (10 $\mu\text{g}/\text{mL}$) for 60 min, followed by VEGF treatment (20 ng/mL) for 60 min. The cells were then fixed, and actin was stained with rhodamine–phalloidin.

cortical actin ring (Fig. 5). These compounds exhibited more potent activities than the parent analog **4**.

We further evaluated analogs **21l**, **n** and **r** using an occludin-based assay. In this assay, normal HRECs retain the polygonal shape and the linear pattern of occludin at the cell border and consequently have intact TJs. However, this pattern is disrupted by VEGF treatment [37]. As shown in Figs. 6 and 7, the oxime analogs enhanced the occludin integrity in the VEGF-treated HRECs. These cell-based assay results indicated that the oxime analogs prevent the apoptosis of endothelial cells and consequently maintain the TJs between endothelial cells.

2.2.2. In vivo assay

Based on the results of the cell-based assays, analog **21l** was selected for evaluation of its preventive effect against retinal vascular leakage in an in vivo model. Initially, the prevention of

VEGF-induced permeability by analog **21l** was examined using a mouse model (Fig. 8) because it has been reported that the retinal permeability caused by an increase in VEGF leads to retinopathy in the diabetic mouse model [37]. After 24 h of intravitreal administration of VEGF and analog **21l** in mice, the retinas were isolated, and the extent of extravasation of FITC-dextran was determined by fluorescein angiography. As anticipated, VEGF-induced retinal vascular leakage was hardly observed after co-injection with analog **21l**. Inspired by the results of the VEGF-induced permeability assay, we evaluated the inhibitory activity of analog **21l** against retinal vascular leakage caused by diabetic retinopathy in the diabetic mouse model. Diabetes was induced in mice by daily intraperitoneal injections of streptozotocin (Sigma) for four consecutive days [42]. Three days after the last streptozotocin injection, mice whose blood glucose concentrations exceeded 30 mg/L were used in this experiment. Analog **21l** reduced vascular leakage to the normal

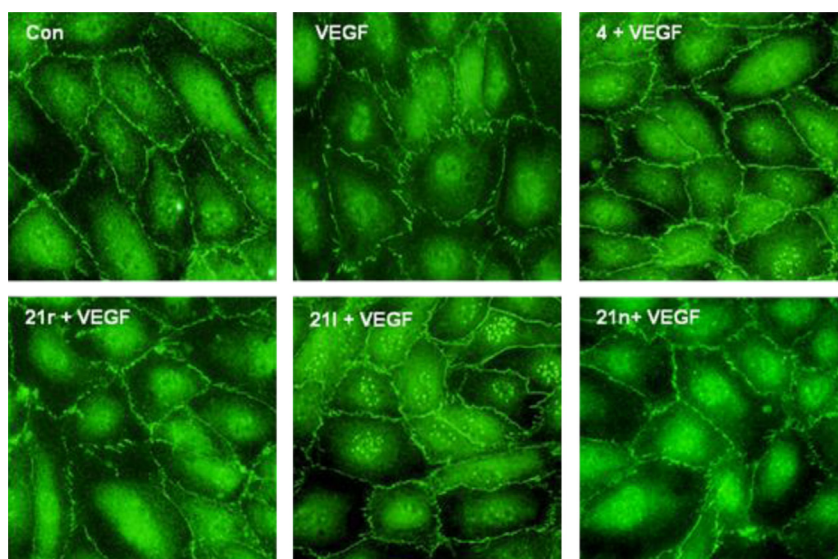


Fig. 6. Changes in the occludin pattern caused by the selected oxime analogs. HRECs were cultured on gelatin-coated dishes for 3 days. The cells were pretreated for 60 min with **21l**, **n**, and **r** (10 $\mu\text{g}/\text{mL}$) then stimulated with VEGF (20 ng/mL) for 60 min. The cells were then fixed, and occludin was labeled with a rabbit-anti-occludin antibody.

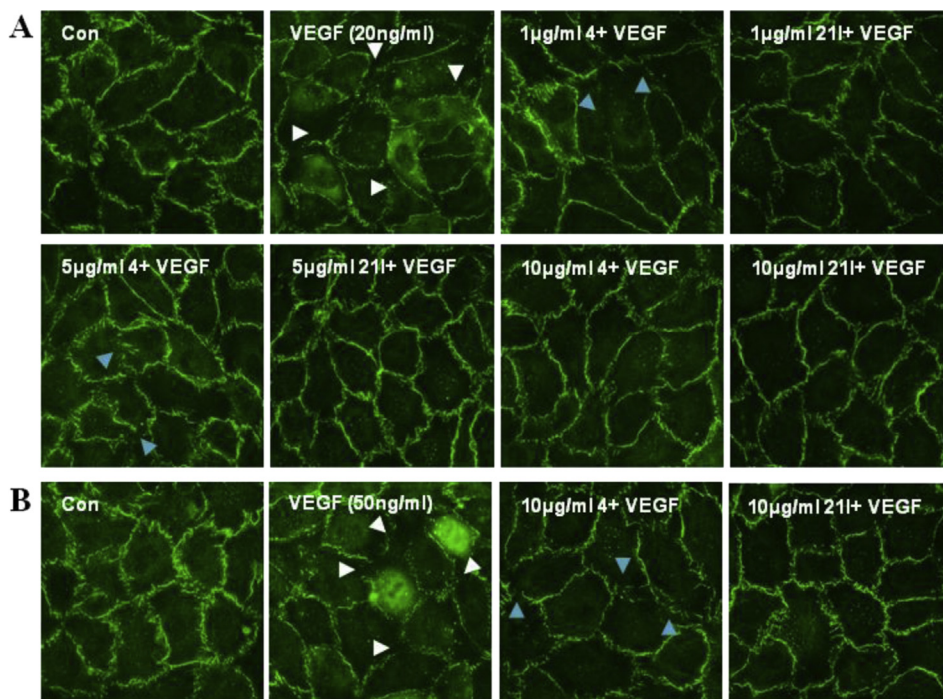


Fig. 7. Changes in the occludin pattern caused by analog **211**. HRECs were grown to confluence and starved with serum free media for 3 h. (A) Cells were treated with various concentration of **4** and **211** for 60 min followed by the stimulation of VEGF (20 ng/mL) for 60 min. (B) Cells were treated with **4** (10 μ g/mL) and **211** (10 μ g/mL) for 60 min followed by the stimulation of VEGF (50 ng/mL) for 60 min. White arrow shows the disruption of the tight junction protein ZO-1 by treatment of VEGF. Blue arrow shows the disruption or disappearance of the ZO-1 staining. (For interpretation of the references to color in this figure legend, the reader is referred to the web version of this article.)

level, as shown in Fig. 9A. In addition, the decreased occludin expression in the retinas of diabetic mice was restored by **211** treatment, as shown in Fig. 9B. Overall, the results of the cell-based and in vivo assays confirmed that analog **211** prevents retinal vessel leakage in a diabetic model as the results of its anti-apoptotic activities and protective effects on TJs.

3. Conclusion

In conclusion, we identified a series of glucal-conjugated sterols with the constrained C₁₇-side chains as novel vascular leakage blocker through design, synthesis and biologically evaluation. Analogs **211**, **n** and **r** exhibited excellent anti-apoptotic activities and TJ protective activities in the in vitro and in vivo models. Among these

compounds, analog **211** was the most potent and exhibited promising in vivo activities for the treatment of vascular disorders. We also established the structure–activity relationship, focusing on the constrained C₁₇-side chains. Currently, further studies on the molecular mechanism and the functional genomics of the sterol analogs are in progress.

4. Experimental protocols

4.1. Chemistry

Unless noted otherwise, all starting materials and reagents were obtained from commercial suppliers and were used without further purification. Tetrahydrofuran and Et₂O were distilled from sodium benzophenone ketyl. Dichloromethane and triethylamine were freshly distilled from calcium hydride. All solvents used for routine isolation of products and chromatography were reagent grade and glass distilled. Reaction flasks were dried at 100 °C before use, and air- and moisture-sensitive reactions were performed under argon atmosphere. Flash column chromatography was performed using silica gel 60 (230–400 mesh, Merck) with the indicated solvents. Thin-layer chromatography was performed using 0.25 mm silica gel plates (Merck). Mass spectra were obtained using a VG trio-2 GC–MS instrument, and high resolution mass spectra were obtained using a JEOL JMS-AX 505WA unit. ¹H NMR spectra were recorded on a JEOL JMS-LA 300, Bruker Analytik ADVANCE digital 400, ADVANCE digital 500 spectrometer in deuteriochloroform (CDCl₃). Chemical shifts are expressed in parts per million (ppm, δ) downfield from tetramethylsilane and are referenced to the deuterated solvent (CHCl₃). ¹H NMR data were reported in the order of chemical shift, multiplicity (s, singlet; d, doublet; t, triplet; q, quartet; m, multiplet and/or multiple resonances), number of protons, and coupling constant in hertz (Hz).

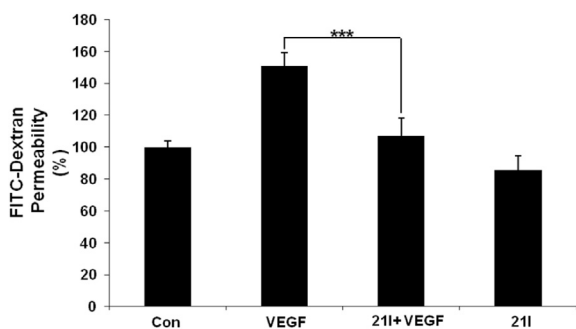


Fig. 8. Inhibitory effect of **211** against VEGF-induced retinal endothelial permeability in a mouse model. VEGF (50 ng) and/or **211** (10 μ g/mL) was intravitreally administered to one eye, and the vehicle (DMSO) with the same total volume of 2 μ L was administered to the contralateral eye. FITC-dextran was injected after 24 h into the ventricle. The level of leakage was quantified using Image J. Permeabilities are presented as the mean \pm S.D.; ****P* < 0.001.

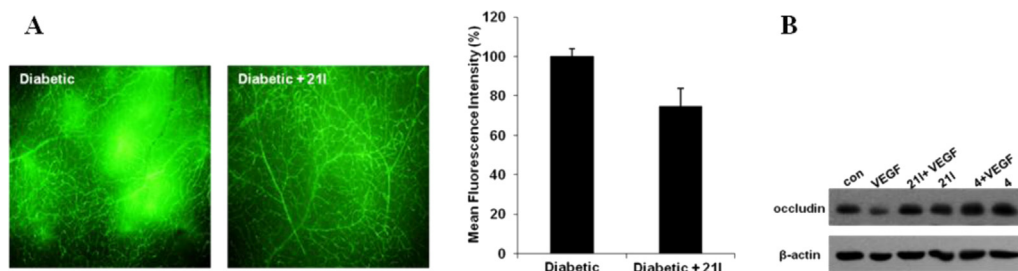


Fig. 9. (A) Effect of **211** on diabetes-induced vascular retinal leakage. Diabetic mice were treated with **211** (10 $\mu\text{g}/\text{mL}$) by intravitreal injection in one eye. The contralateral eye was treated with the same volume (2 μL) of the vehicle (DMSO). FITC-dextran was injected after 24 h into the ventricle, and the retina was photographed. (B) Analog **211** restored the normal occludin level in the eyes of a diabetic mouse, as assessed by Western blot analysis.

4.1.1. Synthetic procedure for the glucal conjugated sterols with modified C_{17} -side chain based on the structures of ginsenosides Rg3 (**1**) and Rk1 (**2**)

4.1.1.1. *(2S)-2-((3S,10R,13S,17S)-10,13-Dimethyl-3-(tetrahydro-2H-pyran-2-yloxy)-2,3,4,7,8,9,10,11,12,13,14,15,16,17-tetradecahydro-1H-cyclopenta[a]phenanthren-17-yl)-6-methylheptan-2-ol* (**5**). To a solution of Magnesium turning (22 mg, 0.92 mmol) with catalytic amount of iodine in diethylether (1 mL) was added 1-bromo-4-methyl pentane (0.17 mL, 1.15 mmol). The reaction mixture was stirred under argon gas until complete consumption of the Magnesium turning at ambient temperature. To a reaction mixture was added **10** (306 mg, 0.76 mmol) in diethylether (1 mL) at ambient temperature. The reaction mixture was stirred until the bubbling was over at ambient temperature. The reaction mixture was quenched with 2 N HCl, and diluted with EtOAc. The organic phase was washed with H₂O and brine, dried over MgSO₄, and concentrated in vacuo. Purification of the residue via flash column chromatography on silica gel (EtOAc:*n*-Hexane = 1:10 to 1:5) afforded 100 mg (27%) of the desired alcohol **5**: ¹H NMR (CDCl₃, 500 MHz) δ 5.33 (t, $J = 6.3$ Hz, 1H), 4.70 (s, 1H), 3.90 (m, 1H), 3.53–3.45 (m, 2H), 2.35–0.82 (m, 49H). HRMS (FAB) calcd for C₃₂H₅₄O₃Na (M + Na⁺): 509.3971. Found 509.3952.

4.1.1.2. *((2R,3S)-3-Acetoxy-6-((3S,10R,13S,17S)-17-((S)-2-hydroxy-6-methylheptan-2-yl)-10,13-dimethyl-2,3,4,7,8,9,10,11,12,13,14,15,16,17-tetradecahydro-1H-cyclopenta[a]phenanthren-3-yloxy)-3,6-dihydro-2H-pyran-2-yl)methyl acetate* (**6**). To a solution of **11** (Fluka, H6378) (43 mg, 0.11 mmol) with tri-*O*-acetyl-*D*-glucal (81 mg, 0.30 mmol) in diethylether (5 mL) was added boron trifluoride diethyl etherate (0.012 mL, 0.10 mmol) at 0 °C. The reaction mixture was stirred for 1 h at ambient temperature. The reaction mixture was quenched with saturated aqueous NaHCO₃ and diluted with EtOAc. The organic phase was washed with H₂O and brine, dried over MgSO₄, and concentrated in vacuo. Purification of the residue via flash column chromatography on silica gel (EtOAc:*n*-Hexane = 1:10) afforded 7.6 mg (12%) of **6**: ¹H NMR (CDCl₃, 500 MHz) δ 5.87–5.79 (dd, $J = 27.1, 10.2$ Hz, 2H), 5.38 (m, 1H), 5.27 (m, 1H), 5.16 (s, 1H), 4.24–4.09 (m, 3H), 3.55 (m, 1H), 2.41–0.76 (m, 47H), 0.69 (d, 1H, $J = 6.75$ Hz), 0.54 (m, 1H). The mass spectral data of analog **6** gives the same value of analog **8**, because of dehydration.

4.1.1.3. *(3S,10R,13S,17S)-17-((S)-2-Hydroxy-6-methylheptan-2-yl)-10,13-dimethyl-2,3,4,7,8,9,10,11,12,13,14,15,16,17-tetradecahydro-1H-cyclopenta[a]phenanthren-3-ol* (**11**). To a solution of Magnesium turning (46 mg, 1.9 mmol) with catalytic amount of iodine in diethylether (1 mL) was added 1-bromo-4-methyl pentane (0.345 mL, 2.37 mmol). The reaction mixture was stirred under argon gas until complete consumption of the Magnesium turning at ambient temperature. To a reaction mixture was added **9** (500 mg, 1.58 mmol) in diethylether (1 mL) at ambient temperature. The

reaction mixture was stirred until the bubbling was over at ambient temperature. The reaction mixture was quenched with 2 N HCl, and diluted with EtOAc. The organic phase was washed with H₂O and brine, dried over MgSO₄, and concentrated in vacuo. Purification of the residue via flash column chromatography on silica gel (EtOAc:*n*-Hexane = 1:10 to 1:5) afforded 96 mg (15%) of the desired alcohol **11**: ¹H NMR (CDCl₃, 300 MHz) δ 5.35 (d, $J = 5.3$ Hz, 1H), 3.53 (m, 1H), 2.32–2.24 (m, 2H), 2.11–0.86 (m, 42H). LR-MS (FAB) m/z 425 (M + Na⁺)

4.1.1.4. *22-((3S,10R,13S,17R)-10,13-Dimethyl-17-(6-methylhept-1-en-2-yl)-2,3,4,7,8,9,10,11,12,13,14,15,16,17-tetradecahydro-1H-cyclopenta[a]phenanthren-3-yloxy)tetrahydro-2H-pyran* (**12**). To a solution of the above alcohol **5** (50 mg, 0.1 mmol) in CH₂Cl₂ (3 mL) was added Et₃N (0.07 mL, 0.5 mmol) and methanesulfonyl chloride (0.015 mL, 0.2 mmol) at 0 °C. The reaction mixture was stirred at 40 °C for overnight. The reaction mixture was quenched with saturated aqueous NaHCO₃ and diluted with CH₂Cl₂. The organic phase was washed with H₂O and brine, dried over MgSO₄, and concentrated in vacuo. Purification of the residue via flash column chromatography on silica gel (EtOAc:*n*-Hexane = 1:20) afforded 18.5 mg (39%) of **12**: ¹H NMR (CDCl₃, 500 MHz) δ 5.34 (m, 1H), 4.84 (s, 1H), 4.74 (s, 1H), 4.70 (m, 1H), 3.90 (m, 1H), 3.53–3.45 (m, 2H), 2.34–0.52 (m, 45H).

4.1.1.5. *(3S,10R,13S,17R)-10,13-Dimethyl-17-(6-methylhept-1-en-2-yl)-2,3,4,7,8,9,10,11,12,13,14,15,16,17-tetradecahydro-1H-cyclopenta[a]phenanthren-3-ol* (**13**). To a solution of the above **12** (18 mg, 0.037 mmol) in MeOH (1.5 mL) was added PTSA (1.9 mg, 0.01 mmol). The reaction mixture was stirred for overnight. The reaction mixture was quenched with H₂O and diluted with EtOAc. The organic phase was washed with H₂O and brine, dried over MgSO₄, and concentrated in vacuo. Purification of the residue via flash column chromatography on silica gel (EtOAc:*n*-Hexane = 1:10) afforded 14 mg (99%) of **13**: ¹H NMR (CDCl₃, 300 MHz) δ 5.34 (m, 1H), 4.79 (d, $J = 28.2$, 1H), 3.51 (m, 1H), 2.25–0.52 (m, 41H). LR-MS (FAB) m/z 385 (M + H⁺).

4.1.1.6. *((2R,3S)-3-Acetoxy-6-((3S,10R,13S,17R)-10,13-dimethyl-17-(6-methylhept-1-en-2-yl)-2,3,4,7,8,9,10,11,12,13,14,15,16,17-tetradecahydro-1H-cyclopenta[a]phenanthren-3-yloxy)-3,6-dihydro-2H-pyran-2-yl)methyl acetate* (**14**). To a solution of the above **12** (18 mg, 0.037 mmol) in MeOH (1.5 mL) was added PTSA (1.9 mg, 0.01 mmol). The reaction mixture was stirred for overnight. The reaction mixture was quenched with H₂O and diluted with EtOAc. The organic phase was washed with H₂O and brine, dried over MgSO₄, and concentrated in vacuo. Purification of the residue via flash column chromatography on silica gel (EtOAc:*n*-Hexane = 1:10) afforded 14 mg (99%) of **13**. To a solution of **13** (16.6 mg, 0.043 mmol) with tri-*O*-acetyl-*D*-glucal (35 mg, 0.13 mmol) in diethylether (2 mL) was added boron trifluoride

diethyl etherate (0.016 mL, 0.13 mmol) at 0 °C. The reaction mixture was stirred for overnight at ambient temperature. The reaction mixture was quenched with saturated aqueous NaHCO₃ and diluted with EtOAc. The organic phase was washed with H₂O and brine, dried over MgSO₄, and concentrated in vacuo. Purification of the residue via flash column chromatography on silica gel (EtOAc:*n*-Hexane = 1:10) afforded 6.9 mg (27%) of **14**: ¹H NMR (CDCl₃, 500 MHz) δ 5.86–5.78 (m, 2H), 5.35 (m, 1H), 5.28–5.13 (m, 3H), 4.24–4.09 (m, 3H), 3.59–3.51 (m, 1H), 2.41–0.52 (m, 46H). HRMS (FAB) calcd for C₃₂H₅₂O₂Na (M + Na⁺): 491.3965. Found 491.3875.

4.1.1.7. 2-((3*S*,10*R*,13*S*,17*R*)-10,13-Dimethyl-17-((*E*)-6-methylhept-2-en-2-yl)-2,3,4,7,8,9,10,11,12,13,14,15,16,17-tetradecahydro-1*H*-cyclopenta[*a*]phenanthren-3-yloxy)tetrahydro-2*H*-pyran (**7**). To a solution of isohexyl triphenylphosphonium bromide (900 mg, 2.1 mmol) in benzene (8 mL) was added potassium *tert*-butoxide 1 M in THF solution (2.1 mL, 2.1 mmol) under Ar atmosphere. The reaction mixture was refluxed for 25 min, then pregnenolone (200 mg, 0.63 mmol) in benzene (2 mL) was added to the solution. The reaction mixture was refluxed for 3 h and cooled to room temperature. Then the reaction mixture was quenched with H₂O and diluted with diethylether. The organic phase was washed with H₂O and brine, dried over MgSO₄, and concentrated in vacuo. Purification of the residue via flash column chromatography on silica gel (EtOAc:*n*-Hexane = 1:10) afforded 54 mg (22%) of the **15**. To a solution of **15** (23 mg, 0.06 mmol) and *p*-toluenesulfonic acid (3 mg, 0.015 mmol) in CH₂Cl₂ (4 mL) was added 3,4-dihydro-2*H*-pyran (0.04 mL, 0.45 mmol) at ambient temperature. The reaction mixture was stirred for 3 h then quenched with H₂O and diluted with EtOAc. The organic phase was washed with H₂O and brine, dried over MgSO₄, and concentrated in vacuo. Purification of the residue via flash column chromatography on silica gel (EtOAc:*n*-Hexane = 1:10) afforded 16 mg (57%) of **7**: ¹H NMR (CDCl₃, 500 MHz) δ 5.33 (t, *J* = 2.4 Hz, 1H), 5.15 (t, *J* = 6.9 Hz, 1H), 4.71 (m, 1H), 3.90 (m, 1H), 3.53–3.45 (m, 2H), 2.34–0.52 (m, 46H). HRMS (FAB) calcd for C₃₂H₅₂O₂Na (M + Na⁺): 491.3965. Found 491.3875.

4.1.1.8. ((2*R*,3*S*)-3-Acetoxy-6-((3*S*,10*R*,13*S*,17*R*)-10,13-dimethyl-17-((*E*)-6-methylhept-2-en-2-yl)-2,3,4,7,8,9,10,11,12,13,14,15,16,17-tetradecahydro-1*H*-cyclopenta[*a*]phenanthren-3-yloxy)-3,6-dihydro-2*H*-pyran-2-yl)methyl acetate (**8**). To a solution of **7** (317 mg, 0.82 mmol) with *tri*-*o*-acetyl-*D*-glucal (672 mg, 2.47 mmol) in diethylether (22 mL) was added boron trifluoride diethyl etherate (0.3 mL, 2.39 mmol) at 0 °C. The reaction mixture was stirred for 3 h at ambient temperature. The reaction mixture was quenched with saturated aqueous NaHCO₃ and diluted with EtOAc. The organic phase was washed with H₂O and brine, dried over MgSO₄, and concentrated in vacuo. Purification of the residue via flash column chromatography on silica gel (EtOAc:*n*-Hexane = 1:10) afforded 270 mg (55%) of **6b**: ¹H NMR (CDCl₃, 500 MHz) δ 5.83 (dd, *J* = 27.3, 10.3 Hz, 2H), 5.34 (t, *J* = 2.3 Hz, 1H), 5.26 (d, *J* = 9.0 Hz, 1H), 5.15–5.14 (m, 2H), 4.25–4.14 (m, 3H), 3.54 (m, 1H), 2.51–0.80 (m, 44H), 0.52 (m, 2H); ¹³C NMR (CDCl₃, 400 MHz) δ 170.8, 170.3, 140.8, 133.9, 128.9, 128.4, 125.8, 121.8, 92.8, 78.1, 66.8, 65.4, 63.2, 58.9, 56.2, 50.4, 43.4, 40.4, 39.2, 38.6, 37.2, 36.8, 32.2, 31.9, 28.2, 27.7, 25.9, 24.7, 24.3, 22.6, 22.5, 21.0, 20.9, 20.8, 19.3, 17.8, 12.9. HRMS (FAB) calcd for C₃₇H₅₆O₆Na (M + Na⁺): 691.3975. Found 691.3961.

4.1.2. General synthetic procedure for preparation of oxime analogs (**21a–r**)

O-Alkyl or aryl hydroxylamine-HCl (1.2 equiv) was added to a solution of **20** (1 equiv) in pyridine (3 mL). The reaction mixture was refluxed for 3 h, cooled to room temperature, and quenched with 2 N HCl, and diluted with diethylether. The organic phase was dried over MgSO₄, and concentrated in vacuo. Purification of the

residue via flash column chromatography on silica gel (EtOAc:*n*-Hexane = 1:10) afforded the corresponding oxime analogs.

4.1.2.1. ((2*R*,3*S*)-3-Acetoxy-6-((3*S*,10*R*,13*S*,17*S*)-17-((*E*)-1-(methoxyimino)ethyl)-10,13-dimethyl-2,3,4,7,8,9,10,11,12,13,14,15,16,17-tetradecahydro-1*H*-cyclopenta[*a*]phenanthren-3-yloxy)-3,6-dihydro-2*H*-pyran-2-yl)methyl acetate (**21a**). Compound **21a** (48 mg, 85%) was afforded from 54 mg of ketone **20**: ¹H NMR (300 MHz, CDCl₃) δ 5.91–5.76 (m, 2H), 5.33 (m, 1H), 5.26 (m, 1H), 5.14 (s, 1H), 4.24–4.07 (m, 3H), 3.80 (s, 3H), 3.58–3.48 (m, 1H), 2.42–0.93 (m, 32H), 0.60 (s, 3H); ¹³C NMR (CDCl₃, 600 MHz) δ 170.8, 170.3, 157.4, 140.8, 128.9, 128.4, 121.6, 92.8, 78.1, 66.8, 65.4, 63.2, 61.1, 56.6, 56.2, 50.2, 43.6, 40.4, 38.6, 37.1, 36.7, 32.0, 31.8, 28.2, 24.2, 23.1, 21.0, 20.9, 20.8, 19.3, 15.6, 13.1. HR-MS (FAB) calcd for C₃₂H₄₈NO₇ (M + H⁺) 558.3431; found 558.3419.

4.1.2.2. ((2*R*,3*S*)-3-Acetoxy-6-((3*S*,10*R*,13*S*,17*S*)-17-((*E*)-1-(ethoxyimino)ethyl)-10,13-dimethyl-2,3,4,7,8,9,10,11,12,13,14,15,16,17-tetradecahydro-1*H*-cyclopenta[*a*]phenanthren-3-yloxy)-3,6-dihydro-2*H*-pyran-2-yl)methyl acetate (**21b**). Compound **21b** (46 mg, 96%) was afforded from 44 mg of ketone **20**: ¹H NMR (300 MHz, CDCl₃) δ 5.91–5.76 (m, 2H), 5.33 (m, 1H), 5.26 (m, 1H), 5.14 (s, 1H), 4.24–4.10 (m, 3H), 4.04 (q, *J* = 20.9 Hz, 2H), 3.56 (m, 1H), 2.42–0.76 (m, 35H), 0.60 (s, 3H); ¹³C NMR (CDCl₃, 400 MHz) δ 170.8, 170.3, 157.0, 140.8, 128.9, 128.3, 121.7, 92.8, 78.1, 68.6, 66.8, 65.4, 63.2, 56.7, 56.2, 50.2, 43.6, 40.4, 38.6, 37.1, 36.7, 32.0, 31.8, 28.2, 24.2, 23.1, 21.0, 20.9, 20.8, 19.3, 15.7, 14.8, 13.2. HR-MS (FAB) calcd for C₃₃H₅₀NO₇ (M + H⁺) 572.3587; found 572.3580.

4.1.2.3. ((2*R*,3*S*)-3-Acetoxy-6-((3*S*,10*R*,13*S*,17*S*)-10,13-dimethyl-17-((*E*)-1-(propoxyimino)ethyl)-2,3,4,7,8,9,10,11,12,13,14,15,16,17-tetradecahydro-1*H*-cyclopenta[*a*]phenanthren-3-yloxy)-3,6-dihydro-2*H*-pyran-2-yl)methyl acetate (**21c**). Compound **21c** (54 mg, 100%) was afforded from 48 mg of ketone **20**: ¹H NMR (300 MHz, CDCl₃) δ 5.91–5.76 (m, 2H), 5.33 (d, *J* = 5.1 Hz, 1H), 5.26 (dd, *J* = 9.2, 1.1 Hz, 1H), 5.15 (s, 1H), 4.25–4.10 (m, 3H), 3.99–3.88 (m, 2H), 3.53 (m, 1H), 2.42–0.82 (m, 37H), 0.60 (m, 3H); ¹³C NMR (CD₃OD, 600 MHz) δ 173.2, 172.8, 159.2, 143.1, 130.6, 130.5, 123.5, 95.0, 80.4, 76.6, 69.2, 67.7, 65.3, 58.7, 58.3, 52.6, 45.7, 42.4, 40.7, 39.3, 38.7, 34.2, 33.7, 30.1, 26.1, 25.0, 24.4, 23.0, 21.6, 21.5, 20.6, 16.8, 14.5, 11.6. HR-MS (FAB) calcd for C₃₄H₅₂NO₇ (M + H⁺) 586.3744; found 586.3734.

4.1.2.4. ((2*R*,3*S*)-3-Acetoxy-6-((3*S*,10*R*,13*S*,17*S*)-17-((*E*)-1-(isopropoxyimino)ethyl)-10,13-dimethyl-2,3,4,7,8,9,10,11,12,13,14,15,16,17-tetradecahydro-1*H*-cyclopenta[*a*]phenanthren-3-yloxy)-3,6-dihydro-2*H*-pyran-2-yl)methyl acetate (**21d**). Compound **21d** (32 mg, 84%) was afforded from 34 mg of ketone **20**: ¹H NMR (300 MHz, CDCl₃) δ 5.91–5.77 (m, 2H), 5.34 (d, *J* = 5.1 Hz, 1H), 5.27 (dd, *J* = 9.4, 1.3 Hz, 1H), 5.15 (s, 1H), 4.31–4.10 (m, 4H), 3.54 (m, 1H), 2.42–0.85 (m, 38H), 0.61 (s, 3H); ¹³C NMR (CDCl₃, 400 MHz) δ 170.8, 170.3, 156.4, 140.8, 128.9, 128.4, 121.7, 92.8, 78.1, 74.2, 66.8, 65.4, 63.2, 56.8, 56.2, 50.2, 43.6, 40.4, 38.6, 37.1, 36.7, 32.0, 31.8, 28.2, 24.3, 23.2, 21.8, 21.7, 21.0, 20.9, 20.8, 19.3, 15.8, 13.2. HR-MS (FAB) calcd for C₃₄H₅₂NO₇ (M + H⁺) 586.3744; found 586.3737.

4.1.2.5. ((2*R*,3*S*)-3-Acetoxy-6-((3*S*,10*R*,13*S*,17*S*)-17-((*E*)-1-(allyloximino)ethyl)-10,13-dimethyl-2,3,4,7,8,9,10,11,12,13,14,15,16,17-tetradecahydro-1*H*-cyclopenta[*a*]phenanthren-3-yloxy)-3,6-dihydro-2*H*-pyran-2-yl)methyl acetate (**21e**). Compound **21e** (63 mg, 86%) was afforded from 66 mg of ketone **20**: ¹H NMR (300 MHz, CDCl₃) δ 5.95 (m, 1H), 5.86–5.76 (m, 2H), 5.33 (m, 1H), 5.28–5.19 (m, 2H), 5.15–5.11 (m, 2H), 4.52–4.50 (m, 2H), 4.24–4.12 (m, 3H), 3.53 (m, 1H), 2.42–0.60 (m, 35H); ¹³C NMR (CDCl₃, 400 MHz) δ 170.8, 170.3, 157.6, 140.8, 134.9, 128.9, 128.4, 121.7, 116.6, 92.8, 78.1, 74.2, 66.8, 65.4, 63.2, 56.7, 56.2, 50.2, 43.6, 40.4, 38.6, 37.1, 36.7, 32.0, 31.8, 28.2,

24.2, 23.1, 21.0, 20.9, 20.8, 19.3, 15.8, 13.2. HR-MS (FAB) calcd for $C_{34}H_{50}NO_7$ ($M + H^+$) 584.3587; found 584.3599.

4.1.2.6. ((2*R*,3*S*)-3-Acetoxy-6-((3*S*,10*R*,13*S*,17*S*)-10,13-dimethyl-17-((*E*)-1-(prop-2-ynoxyimino)ethyl)-2,3,4,7,8,9,10,11,12,13,14,15,16,17-tetradecahydro-1*H*-cyclopenta[*a*]phenanthren-3-yloxy)-3,6-dihydro-2*H*-pyran-2-yl)methyl acetate (**21f**). Compound **21f** (53 mg, 88%) was afforded from 55 mg of ketone **20**: 1H NMR (300 MHz, $CDCl_3$) δ 5.92–5.76 (m, 2H), 5.33 (d, $J = 4.95$ Hz, 1H), 5.26 (m, 1H), 5.15 (s, 1H), 4.61 (d, $J = 2.4$ Hz, 2H), 4.25–4.05 (m, 3H), 3.68–3.41 (m, 1H), 2.42–0.80 (m, 33H), 0.62 (s, 3H); ^{13}C NMR ($CDCl_3$, 400 MHz) δ 170.8, 170.4, 159.1, 140.8, 128.9, 128.4, 121.7, 92.8, 80.5, 78.1, 73.6, 66.8, 65.4, 63.2, 60.8, 56.7, 56.2, 50.2, 43.7, 40.4, 38.6, 37.2, 36.7, 32.0, 31.8, 28.2, 24.2, 23.1, 21.0, 20.9, 20.8, 19.3, 15.9, 13.2. HR-MS (FAB) calcd for $C_{34}H_{48}NO_7$ ($M + H^+$) 582.3431; found 582.3423.

4.1.2.7. ((2*R*,3*S*)-3-Acetoxy-6-((3*S*,10*R*,13*S*,17*S*)-17-((*E*)-1-(butoxyimino)ethyl)-10,13-dimethyl-2,3,4,7,8,9,10,11,12,13,14,15,16,17-tetradecahydro-1*H*-cyclopenta[*a*]phenanthren-3-yloxy)-3,6-dihydro-2*H*-pyran-2-yl)methyl acetate (**21g**). Compound **21g** (44 mg, 88%) was afforded from 44 mg of ketone **20**: 1H NMR (300 MHz, $CDCl_3$) δ 5.33 (d, $J = 5.0$ Hz, 1H) 5.27 (m, 1H), 5.34 (m, 1H), 5.26 (m, 1H), 5.15 (s, 1H), 4.25–4.10 (m, 3H), 4.02–3.97 (m, 2H), 3.59–3.48 (m, 1H), 2.42–0.77 (m, 39H), 0.60 (s, 3H); ^{13}C NMR ($CDCl_3$, 400 MHz) δ 170.8, 170.3, 156.9, 140.8, 128.9, 128.4, 121.7, 92.8, 78.1, 73.0, 66.8, 65.4, 63.2, 56.7, 56.2, 50.2, 43.6, 40.4, 38.6, 37.2, 36.7, 32.0, 31.8, 31.4, 28.2, 24.3, 23.1, 21.0, 20.9, 20.8, 19.3, 19.2, 15.7, 14.0, 13.2. HR-MS (FAB) calcd for $C_{35}H_{54}NO_7$ ($M + H^+$) 600.3900; found 600.3905.

4.1.2.8. ((2*R*,3*S*)-3-Acetoxy-6-((3*S*,10*R*,13*S*,17*S*)-17-((*E*)-1-(isobutoxyimino)ethyl)-10,13-dimethyl-2,3,4,7,8,9,10,11,12,13,14,15,16,17-tetradecahydro-1*H*-cyclopenta[*a*]phenanthren-3-yloxy)-3,6-dihydro-2*H*-pyran-2-yl)methyl acetate (**21h**). Compound **21h** (40 mg, 84%) was afforded from 43 mg of ketone **20**: 1H NMR (300 MHz, $CDCl_3$) δ 5.91–5.76 (m, 2H), 5.33 (d, $J = 5.1$ Hz, 1H), 5.26 (m, 1H), 5.15 (s, 1H), 4.25–4.10 (m, 3H), 3.85–3.71 (m, 2H), 3.53 (m, 1H), 2.42–0.77 (m, 39H), 0.60 (s, 3H); ^{13}C NMR ($CDCl_3$, 600 MHz) δ 170.8, 170.3, 156.9, 140.8, 128.9, 128.4, 121.7, 92.8, 79.9, 78.1, 66.8, 65.4, 63.2, 56.7, 56.2, 50.2, 43.7, 40.4, 38.6, 37.1, 36.7, 32.0, 31.8, 28.2, 28.0, 24.3, 23.1, 21.0, 20.9, 20.8, 19.3, 19.2, 19.2, 15.7, 13.2. HR-MS (FAB) calcd for $C_{35}H_{54}NO_7$ ($M + H^+$) 600.3900; found 600.3917.

4.1.2.9. ((2*R*,3*S*)-3-Acetoxy-6-((3*S*,10*R*,13*S*,17*S*)-10,13-dimethyl-17-((*E*)-1-(pentyloxyimino)ethyl)-2,3,4,7,8,9,10,11,12,13,14,15,16,17-tetradecahydro-1*H*-cyclopenta[*a*]phenanthren-3-yloxy)-3,6-dihydro-2*H*-pyran-2-yl)methyl acetate (**21i**). Compound **21i** (40 mg, 84%) was afforded from 43 mg of ketone **20**: 1H NMR (300 MHz, $CDCl_3$) δ 5.91–5.76 (m, 2H), 5.33 (d, $J = 4.8$ Hz, 1H), 5.25 (m, 1H), 5.15 (s, 1H), 4.24–4.10 (m, 3H), 4.00–3.96 (m, 2H), 3.55 (m, 1H), 2.41–0.76 (m, 41H), 0.60 (s, 3H); ^{13}C NMR ($CDCl_3$, 400 MHz) δ 170.8, 170.3, 157.0, 140.7, 128.9, 128.3, 121.7, 92.8, 78.1, 73.3, 66.8, 65.3, 63.1, 56.7, 56.1, 50.1, 43.6, 40.3, 38.6, 37.1, 36.7, 32.0, 31.8, 28.9, 28.1, 28.1, 24.2, 23.1, 22.5, 21.0, 21.0, 20.8, 19.3, 15.8, 14.0, 13.2. HR-MS (FAB) calcd for $C_{36}H_{56}NO_7$ ($M + H^+$) 614.4057; found 614.4063.

4.1.2.10. ((2*R*,3*S*)-3-Acetoxy-6-((3*S*,10*R*,13*S*,17*S*)-17-((*E*)-1-(isopentyloxyimino)ethyl)-10,13-dimethyl-2,3,4,7,8,9,10,11,12,13,14,15,16,17-tetradecahydro-1*H*-cyclopenta[*a*]phenanthren-3-yloxy)-3,6-dihydro-2*H*-pyran-2-yl)methyl acetate (**21j**). Compound **21j** (48 mg, 100%) was afforded from 41 mg of ketone **20**: 1H NMR (300 MHz, $CDCl_3$) δ 5.91–5.76 (m, 2H), 5.33 (d, $J = 5.0$ Hz, 1H), 5.26 (m, 1H), 5.14 (m, 1H), 4.28–4.12 (m, 3H), 4.02 (t, $J = 13.5$ Hz, 2H), 3.53 (m, 1H), 2.42–0.82 (m, 41H), 0.60 (s, 3H); ^{13}C NMR ($CDCl_3$, 600 MHz) δ 170.8, 170.3, 156.9, 140.8, 128.9, 128.4, 121.7, 92.8, 78.1, 71.8, 66.8, 65.4, 63.2, 56.7, 56.2, 50.2, 43.6, 40.4, 38.6, 38.0, 37.1, 36.7, 32.0, 31.8,

28.2, 25.2, 24.2, 23.1, 22.7, 22.6, 21.0, 20.9, 20.8, 19.3, 15.7, 13.2. HR-MS (FAB) calcd for $C_{36}H_{56}NO_7$ ($M + H^+$) 614.4057; found 614.4035.

4.1.2.11. ((2*R*,3*S*)-3-Acetoxy-6-((3*S*,10*R*,13*S*,17*S*)-10,13-dimethyl-17-((*E*)-1-(3-methylbut-2-enyloxyimino)ethyl)-2,3,4,7,8,9,10,11,12,13,14,15,16,17-tetradecahydro-1*H*-cyclopenta[*a*]phenanthren-3-yloxy)-3,6-dihydro-2*H*-pyran-2-yl)methyl acetate (**21k**). Compound **21k** (49 mg, 80%) was afforded from 53 mg of ketone **20**: 1H NMR (300 MHz, $CDCl_3$) δ 5.91–5.76 (m, 2H), 5.40–5.32 (m, 2H), 5.26 (dd, $J = 9.2, 1.1$ Hz, 1H), 5.14 (s, 1H), 4.50 (d, $J = 7.0$ Hz, 2H), 4.24–4.10 (m, 3H), 3.53 (m, 1H), 2.42–0.76 (m, 38H), 0.60 (s, 3H); ^{13}C NMR ($CDCl_3$, 400 MHz) δ 170.8, 170.3, 157.2, 140.8, 136.9, 128.9, 128.4, 121.7, 120.8, 92.8, 78.1, 70.1, 66.8, 65.4, 63.2, 56.8, 56.2, 50.2, 43.6, 40.4, 38.6, 37.2, 36.7, 32.0, 31.8, 28.2, 25.9, 24.2, 23.1, 21.0, 20.9, 20.8, 19.3, 18.2, 15.8, 13.1. HR-MS (FAB) calcd for $C_{36}H_{54}NO_7$ ($M + H^+$) 612.3900; found 612.3908.

4.1.2.12. ((2*R*,3*S*)-3-Acetoxy-6-((3*S*,10*R*,13*S*,17*S*)-17-((*E*)-1-(cyclopentyloxyimino)ethyl)-10,13-dimethyl-2,3,4,7,8,9,10,11,12,13,14,15,16,17-tetradecahydro-1*H*-cyclopenta[*a*]phenanthren-3-yloxy)-3,6-dihydro-2*H*-pyran-2-yl)methyl acetate (**21l**). Compound **21l** (40 mg, 95%) was afforded from 37 mg of ketone **20**: 1H NMR (300 MHz, $CDCl_3$) δ 5.85 (d, $J = 10.2$ Hz, 1H), 5.80 (d, $J = 10.6$ Hz, 1H), 5.34 (d, $J = 2.6$ Hz, 1H), 5.27 (d, $J = 9.0$ Hz, 1H), 5.15 (s, 1H), 4.61 (m, 1H), 4.24–4.10 (m, 3H), 3.55 (m, 1H), 2.42–0.82 (m, 41H), 0.62 (s, 3H); ^{13}C NMR ($CDCl_3$, 300 MHz) δ 170.8, 170.3, 156.9, 140.8, 128.9, 128.4, 121.7, 92.8, 84.0, 78.1, 66.9, 65.4, 63.2, 56.8, 56.2, 50.2, 43.6, 40.4, 38.7, 37.2, 36.7, 32.2, 32.1, 32.0, 31.8, 28.2, 24.3, 23.9, 23.8, 23.2, 21.0, 20.9, 20.8, 19.3, 15.8, 13.2. HR-MS (FAB) calcd for $C_{36}H_{54}NO_7$ ($M + H^+$) 612.3900; found 612.3901.

4.1.2.13. ((2*R*,3*S*)-3-Acetoxy-6-((10*R*,13*S*,17*S*)-17-((*E*)-1-(cyclohexyloxyimino)ethyl)-10,13-dimethyl-2,3,4,7,8,9,10,11,12,13,14,15,16,17-tetradecahydro-1*H*-cyclopenta[*a*]phenanthren-3-yloxy)-3,6-dihydro-2*H*-pyran-2-yl)methyl acetate (**21m**). Compound **21m** (50 mg, 84%) was afforded from 50 mg of ketone **20**: 1H NMR (400 MHz, $CDCl_3$) δ 5.85 (d, $J = 10.4$ Hz, 1H), 5.80 (m, 1H), 5.34 (s, 1H), 5.27 (d, $J = 9.2$ Hz, 1H), 5.15 (s, 1H), 4.24–4.15 (m, 3H), 4.00 (m, 1H), 3.55 (m, 1H), 2.41–0.84 (m, 42H), 0.61 (s, 3H); ^{13}C NMR ($CDCl_3$, 400 MHz) δ 170.8, 170.3, 156.6, 140.8, 128.9, 128.4, 121.7, 92.8, 79.6, 78.1, 66.8, 65.4, 63.2, 56.9, 56.2, 50.2, 43.7, 40.4, 38.7, 37.2, 36.7, 32.1, 31.9, 31.8, 31.8, 28.2, 25.9, 24.3, 23.9, 23.9, 23.2, 21.0, 21.0, 20.9, 19.3, 15.9, 13.2. HR-MS (FAB) calcd for $C_{37}H_{56}NO_7$ ($M + H^+$) 626.4057; found 626.4050.

4.1.2.14. ((2*R*,3*S*)-3-Acetoxy-6-((10*R*,13*S*,17*S*)-17-((*E*)-1-(cyclohex-2-enyloxyimino)ethyl)-10,13-dimethyl-2,3,4,7,8,9,10,11,12,13,14,15,16,17-tetradecahydro-1*H*-cyclopenta[*a*]phenanthren-3-yloxy)-3,6-dihydro-2*H*-pyran-2-yl)methyl acetate (**21n**). Compound **21n** (47 mg, 80%) was afforded from 50 mg of ketone **20**: 1H NMR (400 MHz, $CDCl_3$) δ 5.90–5.79 (m, 4H), 5.34 (d, $J = 4.7$ Hz, 1H), 5.27 (d, $J = 9.1$ Hz, 1H), 5.15 (s, 1H), 4.56 (br, 1H), 4.24–4.11 (m, 3H), 3.54 (m, 1H), 2.42–0.62 (m, 41H). HR-MS (FAB) calcd for $C_{37}H_{54}NO_7$ ($M + H^+$) 624.3900; found 624.3909.

4.1.2.15. ((2*R*,3*S*)-3-Acetoxy-6-((10*R*,13*S*,17*S*)-17-((*E*)-1-(cyclohexylmethoxyimino)ethyl)-10,13-dimethyl-2,3,4,7,8,9,10,11,12,13,14,15,16,17-tetradecahydro-1*H*-cyclopenta[*a*]phenanthren-3-yloxy)-3,6-dihydro-2*H*-pyran-2-yl)methyl acetate (**21o**). Compound **21o** (50 mg, 82%) was afforded from 50 mg of ketone **20**: 1H NMR (400 MHz, $CDCl_3$) δ 5.86 (d, $J = 10.5$ Hz, 1H), 5.80 (m, 1H), 5.35 (d, $J = 4.9$ Hz, 1H), 5.28 (m, 1H), 5.16 (s, 1H), 4.24–4.14 (m, 3H), 3.86–3.76 (m, 2H), 3.55 (m, 1H), 2.41–0.82 (m, 43H), 0.61 (s, 3H); ^{13}C NMR ($CDCl_3$, 600 MHz) δ 170.8, 170.3, 156.8, 140.8, 128.9, 128.4, 121.7, 92.8, 78.9, 78.1, 66.8, 65.4, 63.2, 56.7, 56.2, 50.2, 43.7, 40.4, 38.7, 37.6, 37.2, 36.7, 32.0, 31.8, 29.9, 29.8, 28.2, 26.7, 25.9, 25.9, 24.3, 23.1, 21.0, 20.9,

20.8, 19.3, 15.7, 13.2. HR-MS (FAB) calcd for C₃₈H₅₈NO₇ (M + H⁺) 640.4213; found 640.4208.

4.1.2.16. ((2*R*,3*S*)-3-Acetoxy-6-((10*R*,13*S*,17*S*)-10,13-dimethyl-17-((*E*)-1-(pyridin-3-ylmethoxyimino)ethyl)-2,3,4,7,8,9,10,11,12,13,14,15,16,17-tetradecahydro-1*H*-cyclopenta[*a*]phenanthren-3-yloxy)-3,6-dihydro-2*H*-pyran-2-yl)methyl acetate (**21p**). Compound **21p** (195 mg, 60%) was afforded from 270 mg of ketone **20**: ¹H NMR (300 MHz, CDCl₃) δ 8.61 (s, 1H), 8.54 (d, *J* = 4.4 Hz, 1H), 7.74 (d, 1H, *J* = 7.7 Hz), 7.32 (m, 1H), 5.90–5.80 (m, 2H), 5.36 (m, 1H), 5.29 (d, *J* = 9.2 Hz, 1H), 5.18 (m, 1H), 5.10 (s, 2H), 4.27–4.10 (m, 3H), 3.56 (m, 1H), 2.40–0.54 (m, 35H); ¹³C NMR (CDCl₃, 500 MHz) δ 170.7, 170.2, 158.5, 149.6, 148.8, 140.7, 135.7, 134.1, 128.8, 128.3, 123.1, 121.6, 92.7, 78.0, 72.6, 66.8, 65.3, 63.1, 56.7, 56.1, 50.1, 43.6, 40.3, 38.6, 37.1, 36.6, 32.0, 31.7, 28.1, 24.1, 23.0, 20.9, 20.9, 20.8, 19.3, 16.0, 13.1. HR-MS (FAB) calcd for C₃₇H₅₁N₂O₇ (M + H⁺) 635.3696; found 635.3701.

4.1.2.17. ((2*R*,3*S*)-3-Acetoxy-6-((3*S*,10*R*,13*S*,17*S*)-17-((*E*)-1-(hydroxyimino)ethyl)-10,13-dimethyl-2,3,4,7,8,9,10,11,12,13,14,15,16,17-tetradecahydro-1*H*-cyclopenta[*a*]phenanthren-3-yloxy)-3,6-dihydro-2*H*-pyran-2-yl)methyl acetate (**21q**). Compound **21q** (43 mg, 74%) was afforded from 43 mg of ketone **20**: ¹H NMR (300 MHz, CDCl₃) δ 5.88 (d, *J* = 10.3 Hz, 1H), 5.79 (m, 1H), 5.33 (d, *J* = 4.8 Hz, 1H), 5.27 (d, *J* = 9.3 Hz, 1H), 5.15 (s, 1H), 4.24–4.10 (m, 3H), 3.54 (m, 1H), 2.42–0.91 (m, 33H), 0.61 (s, 3H); ¹³C NMR (CDCl₃, 600 MHz) δ 170.8, 170.3, 158.7, 140.8, 128.9, 128.4, 121.6, 92.8, 78.1, 66.9, 65.4, 63.2, 56.7, 56.1, 50.2, 43.8, 40.4, 38.6, 37.1, 36.7, 32.0, 31.7, 28.2, 24.2, 23.1, 21.0, 20.9, 20.8, 19.3, 15.1, 13.1. HR-MS (FAB) calcd for C₃₁H₄₆NO₇ (M + H⁺) 544.3274; found 544.3265.

4.1.2.18. ((2*R*,3*S*)-3-Acetoxy-6-((3*S*,10*R*,13*S*,17*S*)-17-((*E*)-1-(benzyloxymino)ethyl)-10,13-dimethyl-2,3,4,7,8,9,10,11,12,13,14,15,16,17-tetradecahydro-1*H*-cyclopenta[*a*]phenanthren-3-yloxy)-3,6-dihydro-2*H*-pyran-2-yl)methyl acetate (**21r**). Compound **21r** (57 mg, 81%) was afforded from 59 mg of ketone **20**: ¹H NMR (300 MHz, CDCl₃) δ 7.34–7.29 (m, 4H), 7.26 (m, 1H), 5.82 (d, *J* = 12.6 Hz, 1H), 5.80 (dt, *J* = 8.2, 1.7 Hz, 1H), 5.34 (m, 1H), 5.26 (dd, *J* = 7.6, 0.8 Hz, 1H), 5.16 (s, 1H), 5.06 (s, 2H), 4.24–4.08 (m, 3H), 3.54 (m, 1H), 2.40–0.82 (m, 32H), 0.56 (s, 3H); ¹³C NMR (CDCl₃, 400 MHz) δ 170.8, 170.3, 157.9, 140.8, 138.7, 128.9, 128.4, 128.2, 127.9, 127.9, 127.4, 121.7, 92.8, 78.1, 75.3, 66.8, 65.4, 63.2, 56.7, 56.2, 50.2, 43.7, 40.4, 38.7, 37.2, 36.7, 32.0, 31.8, 28.2, 24.2, 23.1, 21.0, 21.0, 20.9, 19.4, 16.1, 13.1. HR-MS (FAB) calcd for C₃₈H₅₂NO₇ (M + H⁺) 634.3744; found 634.3727.

4.2. Bioassay material and method

4.2.1. Cell culture

Human retinal ECs (HRECs) were purchased from Applied Cell Biology Research Institute (Kirkland, Wash.) and passages 2–7 were used for experiments. Cells were grown in 2% gelatin-coated dishes and maintained in endothelial cell basal medium (EBM-2, CC-3156) containing EGM-2-kit (CC-4176) (Clonetics, Lonza-Walkersville) and 20% FBS.

4.2.2. Immunofluorescence microscopy

HRECs were fixed in 3.7% formaldehyde for 20 min at room temperature. After fixation, the cells were permeabilized with 0.1% Triton X-100 in phosphate buffered saline for 15 min at 4 °C. Cells were incubated with rabbit anti-occludin antibody (Zymed Laboratories Inc., CA) overnight at 4 °C. The cells were then incubated with Anti-rabbit-Alexa Fluor 488 (Molecular Probes) for 1 h at room temperature. Actin filaments were visualized by staining with rhodamine–phalloidin (Molecular Probes, OR) for 30 min. Cells were mounted using DAKO mounting reagent and observed by fluorescence microscopy (Zeiss; magnification, ×400).

4.2.3. Animals

Eightweeks-old C57BL/6mice (Orient Co., Seoul, Korea) were used for all the experiments. All mice were maintained in a laminar airflow cabinet under specific pathogen-free conditions. They received food and water ad libitum and were maintained on a 12 h alternating light/dark cycle. All facilities are approved by AAALAC (Association of Assessment and Accreditation of Laboratory Animal Care), and all animal experiments were conducted under the institutional guide-lines established for the Animal Core Facility at Yonsei University, College of Medicine, Seoul, Korea.

4.2.4. Diabetic retinopathy mouse model

Diabetes was induced in mice by daily intraperitoneal injection of streptozotocin (Sigma) (90 mg/kg in 0.1 M sodium citrate buffer [pH 4.5]) for 4 consecutive days as modified from Satofuka et al. (2009). The blood glucose level was checked from tail vein blood samples using blood glucose test meter (Gluco Dr™, All Medicus) everyday. Three days after last streptozotocin injection, mice were declared diabetic when the blood glucose concentrations exceeded 300 mg/dl. These mice were intravitreally injected with 1, 5, 10 μg of analog in total volume of 2 μL to one eye and equal volume of vehicle (DMSO) to contralateral eye (*n* = 5/group). 24 h post injection, retina leakage was quantified using fluorescein angiography and Evans blue.

4.2.5. Measurement of retinal leakage using fluorescein angiography and Evans blue

For fluorescein angiography, mice were injected with 3 mg of 40-kDa FITC-dextran (Sigma Aldrich, St Louis, USA) into the left ventricle and the dye was allowed to circulate for 5 min. The eyes were enucleated and immediately fixed in 4% paraformaldehyde for 45 min. The retinas were then dissected out, cut in the Maltese cross-configuration, and flat-mounted onto glass slides. The retinas were viewed under fluorescence microscope (Zeiss; magnification, ×200). Quantification of retinal vascular leakage was done using Evans blue dye as modified from Scheppe et al. (2008). After 24 h of analogs injection, Evans blue (Sigma) was injected into the tail vein of diabetic mice and the dye was allowed to circulate for 1 h. Then, the mice were sacrificed and eyes were immediately enucleated for retina isolation as described above. The dissected retinas were dried in vacuum and weighed. Evans blue dye was extracted from the retinas in formamide (Bioneer; 0.2 mL/retina) at 70 °C for 18 h followed by centrifugation at 14,000 rpm for 60 min. The absorbance of Evans blue dye in the supernatant was measured at 620 nm. Retinal vascular permeability was measured as: [retinal Evans blue concentration (mg/mL)/retinal weight (mg)]/[blood Evans blue concentration (mg/mL) × circulation time (h)].

4.2.6. Western blot analysis

HRECs were lysed in 200 μL RIPA buffer. Lysates were centrifuged at 14,000 rpm for 15 min, and the supernatant was collected. Proteins were separated by 8% sodium dodecyl sulfate–polyacrylamide gel electrophoresis and transferred to nitrocellulose membranes. Membranes were incubated with rabbit anti-occludin antibody (Zymed Laboratories Inc., CA); and goat anti-rabbit-HRP (Thermoscientific, USA) was used as the secondary antibody. Detection was performed with ECL Western blotting detection kit (Amersham, UK) according to the manufacturer's instructions.

4.2.7. Statistical analysis

Data are presented as mean ± S.D, and statistical comparisons between groups were performed by one-way ANOVA followed by Student's *t* test.

Acknowledgments

This work is supported by a grant from the Bio & Medical Technology Development Program of the National Research Foundation of Korea (NRF) funded by the Ministry of Education, Science and Technology (MEST) (NRF-2011-0019267) and by the National Research Foundation of Korea (NRF) grant for the Global Core Research Center (GCRC) funded by the Korea Government (MSIP) (No. 2011-0030001).

Appendix A. Supplementary data

Supplementary data related to this article can be found at <http://dx.doi.org/10.1016/j.ejmech.2014.01.027>.

References

- [1] A.J. Barber, A new view of diabetic retinopathy: a neurodegenerative disease of the eye, *Prog. Neuro-psychopharmacol. Biol. Psychiatry* 27 (2003) 283–290.
- [2] A.J. Barber, E. Lieth, S.A. Khin, D.A. Antonetti, A.G. Buchanan, T.W. Gardner, Neural apoptosis in the retina during experimental and human diabetes. Early onset and effect of insulin, *J. Clin. Invest.* 102 (1998) 783–791.
- [3] A. Bien, C.I. Seidenbecher, T.M. Böckers, B.A. Sabel, M.R. Kreutz, Apoptotic versus necrotic characteristics of retinal ganglion cell death after partial optic nerve injury, *J. Neurotrauma* 16 (1999) 153–163.
- [4] N.A. Maniatis, A. Kotanidou, J.D. Catravas, S.E. Orfanos, Endothelial pathomechanisms in acute lung injury, *Vasc. Pharmacol.* 49 (2008) 119–133.
- [5] P. Libby, Inflammation in atherosclerosis, *Nature* 420 (2002) 868–874.
- [6] S.M. Weis, D.A. Cheresh, Pathophysiological consequences of VEGF-induced vascular permeability, *Nature* 437 (2005) 497–504.
- [7] M. Mizutani, T.S. Kern, M. Lorenzi, Accelerated death of retinal microvascular cells in human and experimental diabetic retinopathy, *J. Clin. Invest.* 97 (1996) 2883–2890.
- [8] L.A. Kerrigan, D.J. Zack, H.A. Quigley, S.D. Smith, M.E. Pease, TUNEL-positive ganglion cells in human primary open-angle glaucoma, *Arch. Ophthalmol.* 115 (1997) 1031–1035.
- [9] K.K. Erickson, J.M. Sundstrom, D.A. Antonetti, Vascular permeability in ocular disease and the role of tight junctions, *Angiogenesis* 10 (2007) 103–117.
- [10] D.S. Fong, L. Aiello, T.W. Gardner, G.L. King, G. Blankenship, J.D. Cavallerano, F.L. Ferris 3rd, R. Klein, Diabetic retinopathy, *Diabetes Care* 26 (2003) s99–s102.
- [11] N.S. Harhaj, D.A. Antonetti, Regulation of tight junctions and loss of barrier function in pathophysiology, *Int. J. Biochem. Cell. Biol.* 36 (2004) 1206–1237.
- [12] J.-K. Min, J.-H. Kim, Y.-L. Cho, Y.-S. Maeng, S.-J. Lee, B.-J. Pyun, Y.-M. Kim, J.H. Park, Y.-G. Kwon, 20(S)-Ginsenoside Rg3 prevents endothelial cell apoptosis via inhibition of a mitochondrial caspase pathway, *Biochem. Biophys. Res. Commun.* 349 (2006) 987–994.
- [13] S. Lee, S. Maharjan, K. Kim, N.-J. Kim, H.-J. Choi, Y.-G. Kwon, Y.-G. Suh, Cholesterol-derived novel anti-apoptotic agents on the structural basis of ginsenoside Rk1, *Bioorg. Med. Chem. Lett.* 20 (2010) 7102–7105.
- [14] S. Maharjan, S. Lee, V. Agrawal, H.-J. Choi, Y.-S. Maeng, K. Kim, N.-J. Kim, Y.-G. Suh, Y.-G. Kwon, SAC-0601 prevents retinal vascular leakage in a mouse model of diabetic retinopathy, *Eur. J. Pharmacol.* 657 (2011) 35–40.
- [15] S. Maharjan, K. Kim, V. Agrawal, H.-J. Choi, N.-J. Kim, Y.-S. Maeng, Y.-G. Suh, Y.-G. Kwon, Sac-1004, a novel vascular leakage blocker, enhances endothelial barrier through the cAMP/Rac/cortactin pathway, *Biochem. Biophys. Res. Commun.* 435 (2013) 420–427.
- [16] S. Lee, S. Maharjan, J.-W. Jung, N.-J. Kim, K. Kim, Y.T. Han, C. Lim, H.-J. Choi, Y.-G. Kwon, Y.-G. Suh, Novel human umbilical vein endothelial cells (HUVEC)-apoptosis inhibitory phytosterol analogues: insight into their structure-activity relationships, *Arch. Pharm. Res.* 35 (2012) 455–460.
- [17] A. Karakurt, M.D. Aytimir, J.P. Stables, M. Özalp, F.B. Kaynak, S. Özbey, S. Dalkara, Synthesis of some oxime ether derivatives of 1-(2-naphthyl)-2-(1,2,4-triazol-1-yl)ethanone and their anticonvulsant and antimicrobial activities, *Arch. Pharm. Chem. Life Sci.* 339 (2006) 513–520.
- [18] Y.-G. Suh, N.-J. Kim, B.-W. Koo, K.-O. Lee, S.-H. Moon, D.-H. Shin, J.-W. Jung, S.-M. Paek, D.-J. Chang, F. Li, H.-J. Kang, T.V.T. Le, Y.N. Chae, C.Y. Shin, M.-K. Kim, J.I. Lim, J.-S. Ryu, H.-J. Park, Design, synthesis, and biological evaluation of novel constrained meta-substituted phenyl propanoic acids as peroxisome proliferator-activated receptor alpha and gamma dual agonists, *J. Med. Chem.* 51 (2008) 6318–6333.
- [19] S.A. Khan, A.M. Asiri, K. Saleem, Synthesis and biological evaluation of new oxime-ether derivatives of steroid as anti-bacterial agents, *J. Saudi Chem. Soc.* 16 (2012) 7–11.
- [20] P. Bunyathaworn, S. Boonananwong, B. Kongkathip, N. Kongkathip, Further study on synthesis and evaluation of 3,16,20-polyoxygenated steroids of marine origin and their analogs as potent cytotoxic agents, *Steroids* 75 (2010) 432–444.
- [21] R.J. Ferrier, N. Prasad, Unsaturated carbohydrates. Part IX. Synthesis of 2,3-dideoxy- α -D-erythro-hex-2-enopyranosides from tri-O-acetyl-D-glucal, *J. Chem. Soc.* (1969) 570–575.
- [22] S.R. Schow, T.C. Morris, Utility of the Wittig reaction for the construction of side chains of steroids starting from pregnenolone, *J. Org. Chem.* 44 (1979) 3760–3765.
- [23] J.N. Kim, K.M. Kim, E.K. Ryu, Improved synthesis of n-alkoxyphthalimides, *Synth. Commun.* 22 (1992) 1427–1432.
- [24] H. Palandoken, C.M. Bocian, M.R. McCombs, M.H. Nantz, A facile synthesis of (tert-alkoxy)amines, *Tetrahedron Lett.* 46 (2005) 6667–6669.
- [25] S.K. Lim, M.J. Park, J.C. Lim, J.C. Kim, H.J. Han, G.-Y. Kim, B.F. Cravatt, C.H. Woo, S.J. Ma, K.C. Yoon, S.H. Park, Hyperglycemia induces apoptosis via CB1 activation through the decrease of FAAH 1 in retinal pigment epithelial cells, *J. Cell. Physiol.* 227 (2012) 569–577.
- [26] R.A. Kowluru, Diabetic retinopathy: mitochondrial dysfunction and retinal capillary cell death, *Antioxid. Redox Signal.* 7 (2005) 1581–1587.
- [27] B.-J. Pyun, S. Choi, Y. Lee, T.-W. Kim, J.-K. Min, Y. Kim, B.-D. Kim, J.-H. Kim, T.-Y. Kim, Y.-M. Kim, Y.-G. Kwon, Capsiate, a nonpungent capsaicin-like compound, inhibits angiogenesis and vascular permeability via a direct inhibition of Src kinase activity, *Cancer Res.* 68 (2008) 227–235.
- [28] clog P values were calculated using ChemDraw version 12.0. See Supplementary Table S1.
- [29] See Supplementary Fig. S1.
- [30] D. Mehta, A.B. Malik, Signaling mechanisms regulating endothelial permeability, *Physiol. Rev.* 86 (2006) 279–367.
- [31] M. Campbell, A.T.H. Nguyen, A.-S. Kiang, L.C.S. Tam, O.L. Gobbo, C. Kerskens, S.N. Dhubbhghail, M.M. Humphries, G.-J. Farrar, P.F. Kenna, P. Humphries, An experimental platform for systemic drug delivery to the retina, *Proc. Natl. Acad. Sci. U. S. A.* 106 (2009) 17817–17822.
- [32] D.A. Antonetti, A.J. Barber, L.A. Hollinger, E.B. Wolpert, T.W. Gardner, Vascular endothelial growth factor induces rapid phosphorylation of tight junction proteins occludin and zonula occluden 1. A potential mechanism for vascular permeability in diabetic retinopathy and tumors, *J. Biol. Chem.* 274 (1999) 23463–23467.
- [33] P. Canning, J.V. Glenn, D.K. Hsu, F.-T. Liu, T.A. Gardiner, A.W. Stitt, Inhibition of advanced glycation and absence of galectin-3 prevent blood-retinal barrier dysfunction during short-term diabetes, *Exp. Diabetes Res.* (2007) 51837.
- [34] E.S. Wittchen, J. Haskins, B.R. Stevenson, Protein interactions at the tight junction. Actin has multiple binding partners, and ZO-1 forms independent complexes with ZO-2 and ZO-3, *J. Biol. Chem.* 274 (1999) 35179–35185.
- [35] F. Drees, S. Pokutta, S. Yamada, W.J. Nelson, W.I. Weis, Alpha-catenin is a molecular switch that binds E-cadherin-beta-catenin and regulates actin-filament assembly, *Cell* 123 (2005) 903–915.
- [36] A. Nusrat, M. Giri, J.R. Turner, S.P. Colgan, C.A. Parkos, D. Carnes, E. Lemichez, P. Boquet, J.L. Madara, Rho protein regulates tight junctions and perijunctional actin organization in polarized epithelia, *Proc. Natl. Acad. Sci. U. S. A.* 92 (1995) 10629–10633.
- [37] D.A. Antonetti, A.J. Barber, S. Khin, E. Lieth, J.M. Tarbell, T.W. Gardner, Vascular permeability in experimental diabetes is associated with reduced endothelial occludin content: vascular endothelial growth factor decreases occludin in retinal endothelial cells. Penn State Retina Research Group, *Diabetes* 47 (1998) 1953–1959.
- [38] J.P. Wiebe, A. Kowalik, R.L. Gallardi, O. Egeler, B.H. Clubb, Glycerol disrupts tight junction-associated actin microfilaments, occludin, and microtubules in Sertoli cells, *J. Androl.* 21 (2000) 625–635.
- [39] S. Ishida, T. Usui, K. Yamashiro, Y. Kaji, E. Ahmed, K.G. Carrasquillo, S. Amano, T. Hida, Y. Oguchi, A.P. Adamis, VEGF164 is proinflammatory in the diabetic retina, *Invest. Ophthalmol. Vis. Sci.* 44 (2003) 2155–2162.
- [40] T. Qaum, Q. Xu, A.M. Jousen, M.W. Clemens, W. Qin, K. Miyamoto, H. Hassessian, S.J. Wiegand, J. Rudge, G.D. Yancopoulos, A.P. Adamis, VEGF-initiated blood-retinal barrier breakdown in early diabetes, *Invest. Ophthalmol. Vis. Sci.* 42 (2001) 2408–2413.
- [41] R.A. Costa, R. Jorge, D. Calucci, L.A. Melo Jr., J.A. Cardillo, I.U. Scott, Intravitreal bevacizumab (avastin) for central and hemicentral retinal vein occlusions: IBeVO study, *Retina* 27 (2007) 141–149.
- [42] S. Satofuka, A. Ichihara, N. Nagai, K. Noda, Y. Ozawa, A. Fukamizu, K. Tsubota, H. Itoh, Y. Oike, S. Ishida, (Pro)renin receptor-mediated signal transduction and tissue renin-angiotensin system contribute to diabetes-induced retinal inflammation, *Diabetes* 58 (2009) 1625–1633.